Metal–oxide bilayer Raman scattering in $SrTiO_3$ thin films

Vladimir I. Merkulov,[a] Jon R. Fox, Hong-Cheng Li,[b] Weidong Si, A. A. Sirenko, and X. X. Xi[c]
Department of Physics, The Pennsylvania State University, University Park, Pennsylvania 16802

(Received 16 December 1997; accepted for publication 21 April 1998)

We have used a metal–oxide bilayer Raman scattering technique to study lattice dynamics in $SrTiO_3$ thin films. The $SrTiO_3$ thin films were epitaxially grown on a conducting metal–oxide layer which reflects the exciting laser beam so that it does not enter the $LaAlO_3$ substrate. Raman scattering from the $SrTiO_3$ thin films was clearly observed, including the first-order Raman peaks forbidden by the cubic symmetry in single crystals. We suggest that strain exists in the films, which changes the crystal symmetry and will affect the dielectric properties of the $SrTiO_3$ thin films. © *1998 American Institute of Physics.* [S0003-6951(98)02725-9]

Recently there has been tremendous interest in utilizing ferroelectric thin films, such as thin films of $Ba_{1-x}Sr_xTiO_3$ (BSTO), in frequency or phase agile electronics, for example in tunable microwave filters and phase shifters.[1,2] It is well established that, for single crystal $SrTiO_3$ (STO), the tunability is related to the hardening of the soft modes[3] and multiple-phonon absorption involving the soft modes contributes primarily to the dielectric losses.[4] In ferroelectric thin films the loss is generally higher than in single crystals. In order to optimize the properties of STO thin films, studies of the lattice dynamics involving the soft modes are required. However, although the results for bulk STO and $BaTiO_3$ are well documented (see references quoted in Ref. 2), little has been reported on soft modes in thin films. We are only aware of one infrared measurement of STO films in the spectral range of 425–800 cm^{-1}, which is far above the soft-mode frequency.[5]

It is difficult to measure Raman scattering in transparent thin films because light goes through the film into the substrate, which has much larger scattering volume and therefore its signal dominates in the Raman spectrum. Various enhancement techniques have been used to study Raman scattering in ultrathin films and clusters.[6] In previous Raman studies of ferroelectric thin films, the thin films were grown either on reflective substrates, such as Pt/Si, or on substrates with low Raman activity at the frequency of interest, such as Al_2O_3, $KTaO_3$, and fused quartz.[7,8] But for many applications these are not the substrates of choice and the crystalline quality of the ferroelectric thin films is often compromised.

The optical phonons in bulk STO are Raman inactive due to crystal symmetry. The Raman spectrum of a STO single crystal is due to second-order Raman scattering, in which two phonons are involved in the scattering process.[9] Departure from the cubic symmetry due to possible strain in the thin films can make phonons observable in Raman measurements. Their intensity is expected to be weak and special approaches are required to enhance the Raman signal. In this letter, we present a metal–oxide bilayer Raman scattering technique. In our structures, conducting metal oxides $YBa_2Cu_3O_7$(YBCO) or $SrRuO_3$(SRO)—which are lattice matched to STO crystals—were used as a reflective layer. A schematic of the experimental configuration is shown in Fig. 1. There are two advantages of this technique. First, the conducting layer reflects a substantial part of the laser beam back into the STO film and the rest attenuates quickly within the conducting layer. Therefore Raman scattering from the substrate can be avoided and the signal from the STO film can be confidently detected. Second, in contrast to growing on substrates such as Pt/Si or Al_2O_3, the metal–oxide bilayer technique ensures *high quality* epitaxial growth of the ferroelectric thin films, which is important for probing intrinsic thin film properties by Raman scattering. This technique is versatile because many conducting metal–oxides can be used as a reflective layer. Furthermore, such bilayer structures are similar to those used in tunable microwave devices; therefore the experimental results are more relevant to practical applications. In our studies phonon spectra from high quality crystalline ferroelectric thin films were clearly measured.

The YBCO, SRO, and STO layers were grown by pulsed laser deposition. $LaAlO_3$ (LAO) substrates were used throughout this work. The deposition pressure was 100 mTorr O_2, the laser energy density was about 1.5–3.0 J/cm^2, and the substrate temperature was in the range between 720–800 °C. The as-deposited films were cooled in 200 Torr O_2

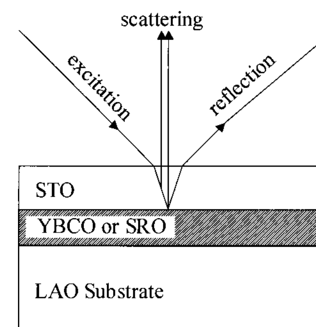

FIG. 1. A schematic of metal–oxide bilayer Raman scattering. The conducting layer ($YBa_2Cu_3O_7$ or $SrRuO_3$) reflects the laser beam so that it cannot reach the $LaAlO_3$ substrate, allowing the study of Raman scattering from the $SrTiO_3$ thin film.

[a]Present address: Oak Ridge National Laboratory, Solid State Division, Oak Ridge, Tennessee 37831.
[b]Also with: National Laboratory for Superconductivity, Institute of Physics, Chinese Academy of Science, Beijing, People's Republic of China.
[c]Electronic mail: xi@phys.psu.edu

 © 1998 American Institute of Physics

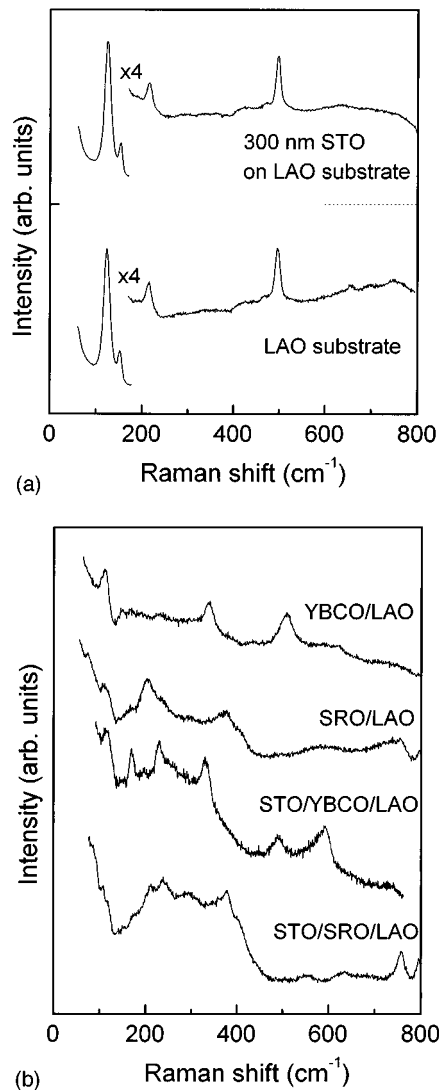

FIG. 2. (a) Raman spectra of a 300 nm $SrTiO_3$ film on a $LaAlO_3$ substrate and a bare substrate. The Raman signal from the substrate overwhelms the Raman spectrum from the $SrTiO_3$ thin film. (b) Raman spectra of a 300 nm $YBa_2Cu_3O_7$ film on a $LaAlO_3$ substrate, a 300 nm $SrRuO_3$ film on a $LaAlO_3$ substrate, a 350 nm $SrTiO_3$ film on $YBa_2Cu_3O_7/LaAlO_3$ substrate and a 350 nm $SrTiO_3$ film on a $SrRuO_3/LaAlO_3$ substrate.

to room temperature. By means of x-ray diffraction we found that both the STO and the conducting layers were grown epitaxially and no other phases have been detected. The Raman spectra were measured at room temperature with a Spex Triplemate spectrometer and an ITT Mepsicron multichannel detector. A 514.5 nm Ar^+ ion laser line was used for excitation. The laser power density was limited to less than 1 W/cm^2 to avoid overheating the sample. A pseudo backscattering geometry was used with an incident angle of about 40°.

In Fig. 2(a) the Raman spectrum of a 350 nm STO thin film deposited on a LAO substrate is shown along with the spectrum of a bare LAO substrate. These two spectra appear identical: they are characterized by the peaks at 125, 154, 216, and 503 cm^{-1}. The Raman features related to the STO thin film cannot be clearly distinguished from the corresponding spectrum because the signal from the substrate overwhelms that from the STO film. The intensity of the substrate spectrum increases with the Raman shift, indicating the further complication that the substrate may be luminescent due to defects within it. From such measurements it is difficult to uniquely obtain a differential spectrum as proposed in Ref. 8.

To block the signal from the substrate, 300 nm conducting YBCO or SRO layers were deposited between the STO film and the LAO substrate. Figure 2(b) shows the Raman spectra of a 300 nm YBCO and a 300 nm SRO film grown on LAO substrates. In these spectra the Raman intensity is much weaker than that from the substrate, and the Raman lines typical for LAO cannot be seen. This shows that the 300 nm conducting films are thick enough to effectively eliminate Raman signal from the substrate. The YBCO film shows Raman peaks at 110, 336, 510, and around 600 cm^{-1}, in agreement with the reported YBCO results.[10] The spectrum of the SRO film has strong peaks at 110, 206, 373, and around 750 cm^{-1}, consistent with the previous report on this material.[11]

Raman spectra of 350 nm STO films grown on reflective layers are also plotted in Fig. 2(b). We compare the spectra of these samples to identify features related to the STO films much as the difference spectrum technique of Ref. 8. The difference between the two techniques is that the Raman signal from the substrate is absent from our spectra. We found that the Raman peaks at 336, 510 and 600 cm^{-1} in the spectrum of STO/YBCO/LAO are due to the YBCO layer, as these peaks were not present in the spectrum of STO/SRO/LAO. On the other hand, the peaks at 212, 377, and 757 cm^{-1} in the spectrum of STO/SRO/LAO are due to the SRO layer, which was not present in the spectrum of STO/YBCO/LAO. The peak at around 110 cm^{-1} could be due to either YBCO or SRO, or STO, and we were not able to unambiguously identify its origin. Excluding these peaks from the spectra, the remaining features are then attributed to the STO thin films. Clearly, the reflective layer has enabled us to observe these peaks which were not distinguishable in STO films deposited directly on the LAO substrate.

Figure 3 shows Raman spectra for STO films of different thickness plotted together with that of a single crystal. The peak at 251 cm^{-1} in the spectrum of bulk STO has been attributed to two-phonon scattering involving the soft-mode phonon and a transverse acoustic phonon.[9] The 228 cm^{-1} feature in the spectra of STO film seems to be also related to this second-order Raman process. Moreover, in the STO thin films we found peaks that could be identified with the first-order Raman process. In the 1000 nm thick STO film, these peaks appear at 168 and 535 cm^{-1}. Their intensities depend on the film thickness. Thus, in the 350 nm STO film, no peak at 535 cm^{-1} was observed. In the even thinner 100 nm STO film, the peak at 168 cm^{-1} disappeared. According to the hyper-Raman scattering result for single crystals, STO has optical phonons at 88 (TO1), 175 (LO1, TO2), 474 (LO3), 545 (TO4), and 795 (LO4) cm^{-1},[12,13] where TO stands for transverse optical and LO for longitudinal optical branches and the numbering of the modes is in order of increasing frequencies. Thus, in our spectra the peaks at 168 and 535 cm^{-1} can be attributed to the scattering by the 175 cm^{-1} LO1 and TO2 and 545 cm^{-1} TO4 bulk phonons, respectively, both of which are symmetry forbidden in the single-crystal spectrum. The broad feature at 560–800 cm^{-1} in the

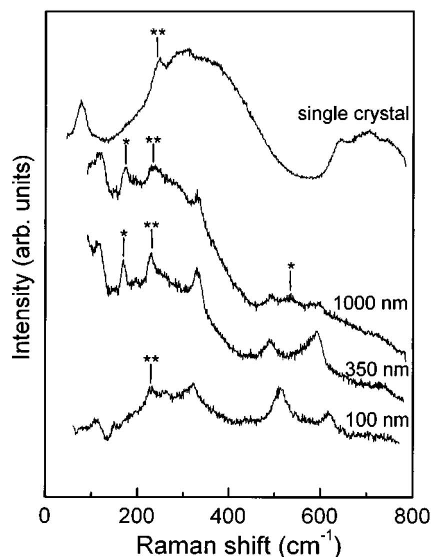

FIG. 3. Raman spectra of a bulk $SrTiO_3$ single crystal and bilayer structures with $SrTiO_3$ films of different thickness (1000, 350, and 100 nm) on a $YBa_2Cu_3O_7/LaAlO_3$ substrate. Peaks unique to STO films are marked with a single asterisk. Double asterisks identify peaks attributed to two-phonon scattering.

single crystal is not observed in the thin films. Due to strong stray light, we were not able to observe features below 100 cm^{-1} in thin film samples. Effort is being made to improve smoothness of the sample surface and extend the measurement range to lower frequencies.

The observation of first-order Raman scattering peaks in the thin films is likely due to strain that changes the crystal symmetry, thus making the Raman-inactive phonons visible. The strain is present even in the thickest film measured, indicating that it is likely local strain caused by the nonequilibrium thin film deposition process. This is supported by the dielectric measurement, in which strain-induced ferroelectricity was observed even in a 2500 nm thick STO film.[14] When the film thickness decreases, the crystallinity of the film improves as evidenced by a general trend in the x-ray rocking curves that the full width at half maximum (FWHM) decreases when the film thickness decreases. For example, a 2500 nm thick film STO film showed a FWHM of 0.46° while it was 0.40° for a 400 nm thick film. Further, in thick STO films weak diffraction from grains of other orientations was often observed, which was absent in the thinner films. Consequently, the 350 nm film shows better-defined peaks than in the 1000 nm film. However, lower film thickness also reduces the signal intensity, causing some peaks to be too weak for detection. Frequencies of the first-order Raman peaks of the STO films decrease with respect to their bulk values by several cm^{-1}. Note that this shift is of the order of the line width at the half maximum. We suggest that the thin film phonons can be affected by lattice distortion around unavoidable symmetry-breaking defects, such as oxygen vacancies, which is the subject of further studies.

In summary, a metal–oxide bilayer Raman scattering technique has been used to study transparent high quality epitaxially grown STO thin films. This technique allows the study of the lattice dynamics in ferroelectric films, such as the effects of thickness, defects, strain, etc. on temperature and electric field dependence of the soft-mode frequency. Utilizing this technique, we found that strain exists in our samples. In order to reduce strain, we have recently grown STO films on better lattice-matched SRO layers and achieved a significant improvement in the loss properties in STO films. A near single-crystal-level low dielectric loss was observed in a 2500 nm thick film STO film.[14] Further enhancement of the Raman signal from transparent films could be made by constructive interference in trilayer resonator structures, or by using a waveguide structure.[6] These approaches are currently being investigated.

This work is partially supported by the NRL SPAWAR program, by the NSF under Grant Nos. DMR-9623889, DMR-9702632 and DMR96-23315, and by the DOE under Grant. No. DE-FG02-84ER45095. The advice from the late Jeffrey S. Lannin at the start of this work is greatly appreciated.

[1] C. M. Jackson, J. H. Kobayashi, D. Durand, and A. H. Silver, Microwave J. **33**, 72 (1992); O. G. Vendik, L. T. Ter-Martirosyan, A. I. Dedyk, S. F. Karmanenko, and R. A. Chakalov, Ferroelectrics **144**, 33 (1993); A. M. Hermann, D. Galt, J. Cuchario, and R. K. Ahrenkiel, J. Supercond. **7**, 463 (1994).
[2] X. X. Xi, in *Laser Applications in Microelectronics and Optoelectronic Manufacturing II*, edited by Jan J. Dubowski, SPIE (SPIE, Bellingham, WA, 1997), Vol. 2991, p. 255.
[3] P. A. Fleury and J. M. Worlock, Phys. Rev. **174**, 613 (1968).
[4] A. K. Tagantsev, in *Ferroelectric Ceramics*, edited by N. Setter and E. L. Colla (Birkhäuser, Basel, Germany, 1993), p.127.
[5] C. H. Mueller, D. Galt, R. E. Treece, T. V. Rivkin, J. D. Webb, H. R. Moutiho, M. Dalberth, and C. T. Rogers, IEEE Trans. Appl. Supercond. **7**, 1628 (1997).
[6] W. S. Bacsa and J. S. Lannin, Appl. Phys. Lett. **61**, 19 (1992); A. Fainstein, M. P. Chamberlain, M. Cardona, K. Toetemeyer, and K. Eberl, Phys. Rev. B **51**, 14 448 (1995).
[7] I. Taguchi, A. Pigonet, L. Wang *et al.*, J. Appl. Phys. **73**, 394 (1993); L. H. Robins, D. L. Kaiser, L. D. Rotter *et al.*, *ibid.* **76**, 7487 (1994); H. Zhang, S. Leppävuori, P. Karjalainen *et al.*, *ibid.* **77**, 2691 (1995); E. Ching-Prado, J. Cordero, and R. S. Katiyar, J. Vac. Sci. Technol. A **14**, 762 (1996).
[8] Z. C. Feng, B. S. Kwak, A. Erbil, and L. A. Boatner, Appl. Phys. Lett. **62**, 349 (1993).
[9] W. G. Nilsen and J. G. Skinner, J. Chem. Phys. **48**, 2240 (1968).
[10] C. Thomsen and M. Cardona, in *Physical Properties of High Temperature Superconductors I*, edited by D. M. Ginsberg (World Scientific, Singapore, 1989), p. 409.
[11] D. Kirillov, Y. Suzuki, L. Antognazza, K. Char, I. Bozovic, and T. H. Geballe, Phys. Rev. B **51**, 12 825 (1995).
[12] V. N. Denisov, B. N. Mavrin, and V. B. Podobedov, Phys. Rep. **151**, 1 (1987).
[13] H. Vogt and G. Rossbroich, Phys. Rev. B **24**, 3086 (1981); H. Vogt, *ibid.* **38**, 5699 (1988).
[14] H.-C. Li, W. Si, A. D. West, and X. X. Xi, Appl. Phys. Lett. (to be published).